Journal of Rare Cardiovascular Diseases

ISSN: 2299-3711 (Print) | e-ISSN: 2300-5505 (Online)



RESEARCH ARTICLE

A Medical Expert System for the Diagnosis of Cardiovascular Disease using Integrated DI-LSTM and T-ANFIS Rule-Based Models

Mathan S1 and Sunil Gupta2

¹Research Scholar, School of Computer and Systems Sciences, Jaipur National University, Jaipur, Rajasthan, India. ²Professor, HOD School of Computer and Systems Sciences, Jaipur National University, Jaipur, Rajasthan, India.

*Corresponding Author Mathan S (mathansj@outlook.com)

Article History

Received: 14.07.2025 **Revised:** 22.08.2025 **Accepted:** 19.09.2025 **Published:** 04.10.2025

This research presents a deep learning framework for the diagnosis of heart disease. Abstract: The proposed model combines a Dropout-layer Induced Long Short-Term Memory (DI-LSTM) network with a Trapezoidal-based Adaptive Neuro-Fuzzy Inference System (T-ANFIS). The objective of this combination is to improve the computational efficiency and the diagnostic accuracy. Firstly, the ECG signals pre-processed and decomposed by removing baseline drift and smoothing. Then the most relevant features such as statistical properties, time-related factors, amplitude measurements, and pulse characteristics are extracted. We optimize these features with a Dent Map-based Red Fox Optimization (TM-RFO) algorithm, which improves search capabilities and avoids getting stuck in local minima by using Dent Map dynamics. The improved feature set is fed into a DI-LSTM framework. Dropout layers are used to improve generalization and prevent overfitting. This allows for binary classification of signals as normal or abnormal. If signals are abnormal, they go through a secondary classification using the T-ANFIS framework. To handle complex data patterns and identify conditions such as atrial fibrillation (AFib), ventricular fibrillation (VFib), and bradycardia, we use structural adaptive trapezoidal membership functions. Our framework shows that it performs better in terms of sensitivity, specificity, recall, accuracy, and precision metrics compared to existing methods.

Keywords: Dropout-layer Induced Long Short-Term Memory, Tent Map-based Red Fox Optimization, Trapezoidal Adaptive Neuro-Fuzzy Inference System, deep neural network, Cardiac Disease Diagnosis.

INTRODUCTION

The major cause of death globally is cardiovascular diseases (CVDs), which are responsible for millions of deaths annually [1]. The diagnosis of heart conditions has traditionally relied on electrocardiogram (ECG) signals, and better patient outcomes depend on the early identification and management of these conditions. ECGs provide a non-invasive way to record the electrical activity of the heart and are essential for detecting abnormalities such as arrhythmias, myocardial infarctions, and other cardiac dysfunctions [2]. Cardiologists' manual interpretation is the mainstay of conventional ECG analysis methods, which can be timeconsuming and prone to human error [3]. However, in recent years, there has been a noticeable trend toward automating this process through the use of deep learning (DL) and machine learning (ML) technologies, which have demonstrated great promise in enhancing the accuracy and efficacy of cardiac detection systems [4]. These sophisticated computational methods use algorithms to filter and analyze large, complicated datasets, revealing aspects and patterns that human observers might not see right away.

A cardiac diagnosis system that incorporates ML and DL models can vastly improve the diagnostic workflow. The process begins with data acquisition, where ECG signals are captured from patients using sensors and other monitoring devices. Due to several variables, including patient mobility and interference from other electronic

devices, this raw data frequently contains noise and artifacts [5]. To guarantee that only pertinent data is input into the algorithms, preprocessing is therefore an essential step that entails removing noise and standardizing the data. Once the data is preprocessed, feature extraction is performed to identify key characteristics of the ECG signals that are indicative of specific cardiac conditions. Traditionally, this involved manual extraction of features like heart rate, QRS complex duration, and ST segment deviation. However, with deep learning, feature extraction can be automated, allowing models to learn and identify complex features directly from the data [6].

The classification of ECG signals has heavily relied on machine learning techniques including k-nearest neighbors (KNN), random forests, and support vector machines (SVM). SVM operates by determining the best hyperplane to divide various data classes, and it is very useful for binary classification applications. While random forests are resistant to overfitting, they are ensemble approaches that use several decision trees to handle high-dimensional data and enhance classification accuracy [7]. KNN classifies data points based on their proximity to other labeled data points, and while simple, it can be effective in distinguishing between different types of arrhythmias. Despite their effectiveness, these traditional ML algorithms require manual feature engineering and are often limited in their ability to handle complex, high-dimensional data [8].



Deep learning models come into play here, offering significant advantages over traditional methods. For example, Convolutional Neural Networks (CNNs) are particularly well-suited for processing and evaluating ECG signals because they can automatically learn hierarchical properties from raw data. To accurately categorize cardiac illnesses, CNNs are composed of multiple layers that recognize patterns [8], such as shapes, edges, and higher-level characteristics. Because they are designed to handle sequential data, recurrent neural networks (RNNs), including Long Short-Term Memory (LSTM) networks, are ideal for processing time-series data, including ECG signals. The ability of LSTMs to identify patterns over time and capture longterm interdependence is crucial for diagnosing illnesses with temporal variability [9].

Deep learning techniques like autoencoder are employed for unsupervised learning tasks like dimensionality reduction and feature extraction. They acquire condensed representations of ECG signals, which can subsequently be applied to tasks involving anomaly detection or classification [10]. Deep learning models' automatic feature extraction capabilities lessen the need for human input and make it possible to find intricate linkages and subtle patterns in the data. Deep learning models are also very useful tools in the context of cardiac diagnostics since they can be trained on vast datasets to increase their prediction accuracy and generalization skills [11].

Heart disease datasets are crucial for the creation and evaluation of these complex cardiac detection algorithms. These sets often include annotated electrocardiograms from both healthy individuals and patients with various heart conditions. Cardiology Challenge PhysioNet/Computing in databases, the MIT-BIH Arrhythmia Database, and the PTB Diagnostic ECG Database are just a few of the wellknown datasets that researchers can use to train and test machine learning models [12]. The MIT-BIH Arrhythmia Database, for instance, has over 48 half-hour snippets of two-channel ambulatory ECG recordings that are labeled with various types of arrhythmias to develop robust classification algorithms. The availability of such extensive datasets makes it possible to rigorously test and validate machine learning models, guaranteeing their correctness and dependability in actual clinical settings.

There are many advantages of integrating ML and DL in cardiac diagnostic systems. First of all, by analyzing ECG signals almost instantly, these devices can drastically cut down on the amount of time needed for diagnosis and facilitate quicker clinical decision-making. In emergency cases where prompt diagnosis and treatment are crucial, this is especially crucial [13]. Second, the computerized analysis frees up medical staff to concentrate on more complicated cases that call for human knowledge. Furthermore, by improving diagnostic precision, deep learning and machine learning

models can reduce the likelihood of misdiagnosis and false positives. These tools improve the accuracy of cardiac diagnosis, which eventually improves patient outcomes, by spotting minute patterns and abnormalities that human observers might miss. But putting these technologies into practice is not without its difficulties. Access to sizable, superior datasets that are representative of many patient populations is necessary for the creation of successful machine-learning models [14]. Another big worry is making sure that data is secure and private, especially when it comes to private medical data. The incorporation of models based on machine learning and deep learning into the existing healthcare infrastructure requires thorough evaluation and coordination by technology developers, clinicians, and regulatory bodies to ensure seamless adoption and conformity to medical norms [15]. Despite these challenges, ML for cardiac diagnostics have huge potential benefits, and more research and development in this field should lead to significant advancements in the diagnosis and treatment of heart diseases. The main contributions of this study are summarized as follows:

- This work combines a deep neural network uses DI-LSTM model and T-ANFIS, leveraging the strengths of both models for accurate and efficient cardiac disease diagnosis from ECG signals.
- TM-RFO is used to identify features efficiently, enhance exploration, and stay clear of local optima.
- To improve generalization and decrease overfitting when classifying ECG signals as normal or abnormal, the DI-LSTM network is implemented.
- The suggested model performs better than current methods, categorizing cardiac diseases with greater accuracy, precision, recall, sensitivity, and specificity.

The document's remaining sections are organized as follows. Cardiovascular disease prediction was covered in Section 2. Section 3 describes the proposed T-ANFIS model. Section 4 presents the results of experiments conducted using the datasets. Section 5 concludes the current study work.

Related work

Karthik et al. [16] developed an automated algorithm based on deep learning for identifying 1D bio ECG signals to diagnose cardiovascular disease. The DLECG-CVD model has several operational steps, including preprocessing, feature extraction, hyperparameter tuning, and classification. Data pre-processing is the initial step in transforming the ECG results into actionable information and getting them ready for further analysis. A deep belief network (DBN) model is then used to produce a set of feature vectors. To optimize the hyperparameters of the DBN model, the Improved Swallow Swarm Optimization (ISSO) technique is employed. Lastly, the test ECG data is given the proper class labels using the Extreme Gradient Boosting



classifier. The benchmark PTB-XL dataset was used in simulations to validate the improved diagnostic performance of the DLECG-CVD model. The model showed gains in kappa, Matthew correlation coefficient, accuracy, sensitivity, specificity, and hamming loss after a thorough comparison examination.

Abubaker et al. [17] created a new lightweight CNN design that outperformed current state-of-the-art techniques in cardiovascular disease categorization, increasing the accuracy rate to 98.23%. The model may run on a single CPU, circumventing computing power constraints, and this was accomplished using a collection of ECG scans from cardiac patients. Furthermore, a significant improvement in classification accuracy was obtained when the proposed method was used as a feature extraction tool for traditional machine learning techniques. For instance, the Naïve Bayes algorithm achieved an accuracy of 99.79%. This approach can be included in the healthcare IoT ecosystem, encouraging other AI researchers to look at cutting-edge methods for cardiovascular disease diagnostics.

Mhamdi et al. [18] created algorithmic models for analyzing ECG tracings to predict cardiovascular disorders to save lives and enhance healthcare at a reduced cost. As the cost of healthcare and insurance rises globally, this work holds enormous promise for offering life-saving and reasonably priced solutions. A validation accuracy of approximately 0.95 was attained by the MobileNetV2 and VGG16 algorithms following a thorough testing process to adjust deep learning settings. Accuracy marginally dropped to 0.94 and 0.90 when MobileNetV2 and VGG16 were installed on a Raspberry

Pi. The primary objective of this study was to enhance real-time monitoring easily and economically using smart mobile technologies such as smartphones, smartwatches, and connected T-shirts.

Daydulo et al. [19] created an automated deep-learning algorithm that can correctly categorize ECG data into three groups: cardiac arrhythmia (ARR), congestive heart failure (CHF), and normal sinus rhythm (NSR). This was accomplished by pre-processing and segmenting ECG data from the MIT-BIH and BIDMC databases that are accessible on PhysioNet before the model being trained. Pre-trained models, including ResNet 50 and Alex Net, were set up and tweaked to provide the best classification results. The proposed deep learning model demonstrated an overall classification accuracy of 99.2% on the test data, with an average sensitivity of 99.2%, specificity of 99.6%, and precision, F-measure, and recall of 99.2%.

Ram et al. [20] used three deep learning models—Multilayer Perceptron's (MLPs), Deep Belief Networks (DBNs), and Restricted Boltzmann Machines (RBMs)—as well as electrocardiogram (ECG) signals as the main data source in order to identify heart disorders. Their model was trained and evaluated using the MIT-BIH and PTB-ECG datasets, which are both publically available. In comparison to earlier models, the hybrid model demonstrated remarkable accuracy, achieving 98.6%, 97.4%, and 96.2% on the MIT-BIH dataset and 97.1%, 96.4%, and 95.3% on the PTB-ECG dataset, respectively. Furthermore, the robustness of the suggested method was shown by high F1 scores and AUC values.

Problem statement

- The identification and separation of distinct heart disease types is a crucial gap in many current approaches used in the context of cardiac illness detection systems. The accuracy and efficacy of diagnosis and therapy may be severely impacted by this disparity.
- Existing heart disease diagnosis systems may struggle with accurate classification due to their inability to effectively handle and integrate different types of datasets.
- The existing systems may not effectively select and prioritize relevant features from diverse datasets, leading to the inclusion of irrelevant or redundant features that adversely affect model performance.
- Multiple sources of high-dimensional data may cause overfitting, in which the classification model picks up noise
 and particular training data patterns instead of broadly applicable patterns. When applied to fresh, untested data,
 this leads to decreased accuracy.

Table 1: Evaluation of current methods for diagnosing CVD in comparison

| Author | Dataset | Methods | Accuracy | Limitation | |
|----------------------|--------------------|-----------------|-----------------------|-----------------------------|--|
| Karthik et al. [16] | PTB-XL dataset | DLECG-CVD | The DLECG-CVD | The DLECG-CVD model's | |
| | | model | model achieved a | reliance on the PTB-XL | |
| | | | high accuracy rate in | dataset limits its | |
| | | | diagnosing | generalizability. | |
| | | | cardiovascular | | |
| | | | diseases from ECG | | |
| | | | signals. | | |
| Abubaker et al. [17] | ECG Images | Lightweight CNN | At 98.23%, the | The model's reliance on one | |
| | Dataset of Cardiac | | lightweight CNN | dataset limits its | |
| | Patients | | architecture | applicability to other | |
| | | | obtained a | populations. | |

| | | | remarkable | |
|---------------------|----------------------|-------------------|--------------------|------------------------------|
| | | | accuracy rate. | |
| Mhamdi et al. [18] | Training and testing | Mobile Net V2 and | The proposed model | The model may not perform |
| | dataset | VGG16 algorithms | achieves 95% | effectively for all types of |
| | | | | cardiac arrhythmias. |
| Daydulo et al. [19] | MIT-BIH and | Deep learning | 99.2% accuracy is | Less reliable |
| | BIDMC databases | model | attained with the | |
| | | | deep learning | |
| | | | model. | |
| Ram et al. [20] | MIT-BIH, PTB- | HybDeepNet model | HybDeepNet Model | More diverse datasets |
| | ECG dataset | | achieves an | |
| | | | accuracy of 98.6%. | |
| | | | - | |

Proposed Methodology for Cardiac Disease Diagnosis System

This paper presents an advanced cardiac disease diagnosis system that combines an Enhanced deep neural network using a DI-LSTM network and a T-ANFIS, utilizing patient ECG signals as input. Initially, the ECG signals are decomposed and pre-processed to eliminate baseline wandering and smooth the data, preparing it for beat feature extraction. For feature selection, the system uses the Tent Map-based Red Fox Optimization (TM-RFO) algorithm, which enhances exploration capabilities in complex search landscapes by integrating chaotic dynamics, allowing the algorithm to bypass local optima without relying on gradients. The selected features are then fed into a deep neural network using a DI-LSTM network, tailored for managing sequential data and minimizing overfitting through the random dropout of units during training, which improves generalization. If the model detects an abnormal heartbeat, the data is further analyzed using T-ANFIS. This model leverages adaptive trapezoidal membership functions that fine-tune during training to capture intricate data distributions accurately. T-ANFIS classifies specific cardiac conditions, including Atrial Fibrillation (AFib), Ventricular Fibrillation (VFib), and Bradycardia. The system's performance is evaluated against existing methodologies using various quality metrics. Fig. 1 depicts a block schematic of the suggested approach.

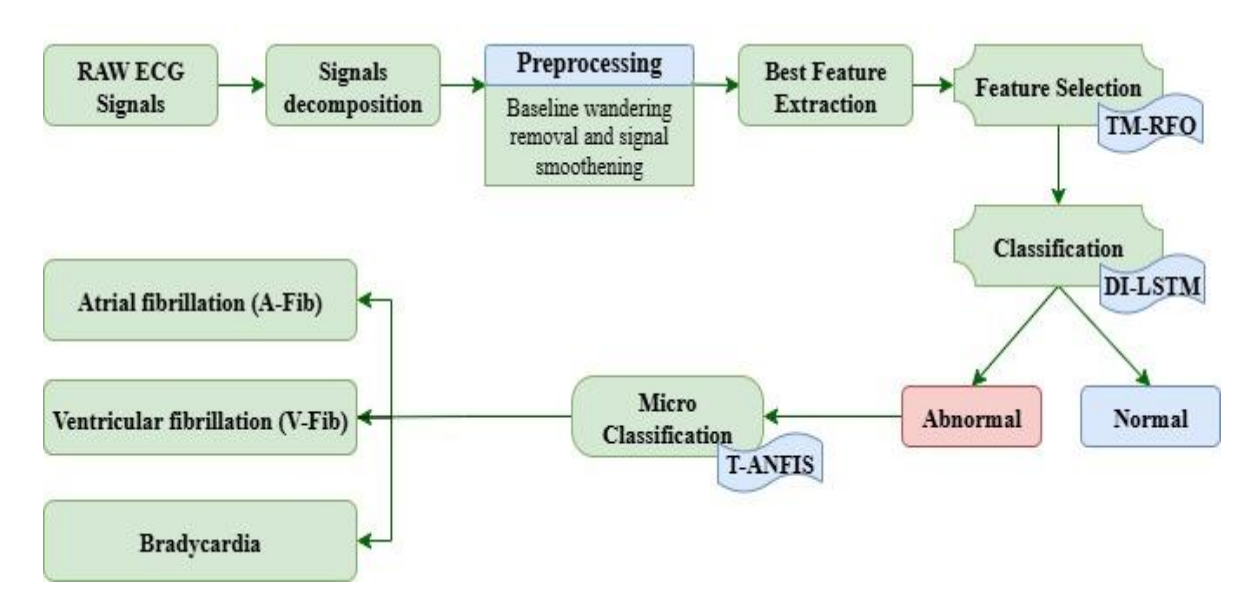


Fig 1: The suggested cardiac disease diagnosis system's block diagram

Raw ECG signals

ECG images from cardiac diseases and raw ECG signals x(t) from the MIT-BIH collection offer a wealth of labeled ECG recordings of the heart's electrical activity throughout time. These signals, which are obtained from patients using conventional electrodes applied to the skin, may contain baseline drift, noise, and artifacts for a variety of causes.

Signal decomposition

The acquired ECG signal x(t) can be decomposed into various components using techniques.

The Hilbert transform is a mathematical operation that transforms a real-valued function (signal) into another function that provides important information about the original signal, specifically its instantaneous amplitude and phase. It is widely



used in signal processing, communications, and various fields of engineering and physics. It x(t) is the input ECG signal, the Hilbert transform H(x(t)) is given by,

$$H(x(t)) = \frac{1}{\pi} P.V. \int_{-\infty}^{\infty} \frac{x(\tau)}{t - \tau} d\tau$$
 (1)

Where P.V denotes Cauchy's principal valuewhich is needed due to the singularity at $t-\tau$, H(x(t)) Hilbert transform x(t).

Pre-processing

In this pre-processing, baseline wandering removal is performed and then the signal is smoothened.

Baseline Wandering Removal

Baseline wandering refers to slow variations in the ECG signal caused by patient movement or respiration, which is removed using a high-pass filter. The cut-off frequency of the filter f_c is typically between 0.5-0.7 Hz to remove low-frequency noise while preserving important ECG features. The high-pass filter function H(f) is expressed as:

$$H(f) = \frac{f}{\sqrt{f^2 + f_c^2}} \tag{2}$$

Where f_c the cut-off frequency of the filter (around 0.5 Hz for ECG), f is the signal frequency, H(f) the frequency response of the filter at frequency f.

Signal Smoothing

After baseline wandering is removed, the ECG signal is further smoothened using a Gaussian filter to remove noise. The Gaussian function is defined as,

$$G(t) = \frac{1}{\sqrt{2\pi\sigma^2}} e^{-\frac{t^2}{2\sigma^2}}$$
 (3)

Where σ is the standard deviation, t is the time variable. Convolving the ECG signal with this filter reduces high-frequency noise while preserving the essential features.

Feature extraction

After pre-processing, beat features (R-peak detection, RR intervals, QRS detection, heart rate variability (HRV), mean and standard of RR intervals), Amplitude features (max amplitude and min amplitude), statistical features (mean, standard deviation, kurtosis and skewness) and time domain features (rms, signal energy and no of peak) and other ECG signal characteristics are extracted. These features form a feature vector F:

$$F = [f_1, f_2,, f_n]$$
(4)

Where f_i represents a specific feature extracted from the ECG signal.

Feature selection using TM-RFO

For this feature selection process, the extracted features F are selected using the TM-RFO algorithm. The existing RFO [21] algorithm is notable for its simplicity and speed, as it does not require gradient information, which distinguishes it from many other optimization methods. However, RFO tends to converge prematurely to local optima, particularly in complex, multimodal landscapes where it can be difficult to differentiate between local and global optima. The proposed TM-RFO is an enhanced optimization technique that integrates the RFO algorithm with the Tent Map to improve the exploration capabilities of the algorithm, especially in complex, multimodal search spaces. To avoid early convergence to local optima, this feature selection approach seeks to identify the most pertinent features from the feature vector.

In feature selection, the goal is to find an optimal subset of features $S \subset X$ from the feature set $X = \{x_1, x_2, x_3, x_n\}$, the objective is to maximize classification performance with the fewest possible features to reduce complexity and increase model interpretability. The optimization is represented by an objective function J(S).

$$\max_{S \subset X} J(S) = Acc(S) - \lambda |S|$$
 (5)



Where |S| several features, λ are a regularization parameter to penalize a larger subset.

Initialize the population of foxes

Each individual in the TM-RFO population, called a fox represents a candidate subset of features, encoded as a binary vector $P_i = [P_{i_1}, P_{i_2}, ..., P_{i_n}]$.

The algorithm initializes a population of N foxes by randomly assigning binary values to the elements in each vector P_i . This random initialization creates diverse candidate solutions, covering different portions of the feature space.

For each fox P_i , the fitness is evaluated using the objective function:

$$J(P_i) = Acc(P_i) - \lambda |P_i| \tag{6}$$

Where $Acc(P_i)$ is the classification performance using the feature represented by P_i , λ is a regularization parameter, and $|P_i|$ is the count of selected features.

Exploitation and Exploration Phases in TM-RFO

The TM-RFO algorithm alternates between two phases' exploitation (local search) and exploration (global search). This alternating approach enables the algorithm to refine promising solutions while exploring the search space broadly to avoid premature convergence.

Exploitation Phase (Local Search)

In the exploitation phase, the algorithm performs a local search around high-fitness solutions. Small changes or "mutations" are made to the fox's position vector P_i , which may involve flipping one or a few bits (i.e., selecting or deselecting a small number of features).

For instance, with a small probability \in , each element p_{ii} is updated as:

$$p_{ij}^{t+1} = \begin{cases} 1 - p_{ij}^{t}, & \text{if a random number} < \epsilon \\ p_{ii}^{t}, & \text{otherwise} \end{cases}$$

$$(7)$$

This local flipping enables minor adjustments around the current subset, allowing the algorithm to fine-tune its selection to improve fitness.

Exploration Phase (Global Search using Tent Map)

In the exploration phase, the algorithm uses the Tent Map to introduce chaotic behavior, enhancing its ability to explore the search space and avoid local optima.

The tent map T(x) is defined as:

$$T(x) = \begin{cases} 2x, & \text{if } 0 \le x < 0.5, \\ 2(1-x), & \text{if } 0.5 \le x \le 1. \end{cases}$$
 (8)

This chaotic function generates values in the interval (0, 1), providing non-linear, unpredictable sequences that enhance global exploration.

Update Positions Using Tent Map Dynamics

The tent map introduces chaotic sequences into the position updates of each fox, facilitating large, random-like jumps in the feature space. $x_{current}$ Represents the current position of the fox, the tent map generates a new value $T(x_{current})$, and the updated position x_{new} is calculated as:

$$x_{new} = x_{current} + \alpha T(x_{current})$$
 (9)

Where α is a scaling factor that controls the influence of the Tent Map on the position update, $x_{current}$ the previous value of the same vector, x_{new} represents the updated or new value of a variable. Since feature selection is binary, the continuous positions generated by the Tent Map are mapped back to binary format by applying a threshold.

$$p_{ij}^{t+1} = \begin{cases} 1 - p_{ij}^{t} & ,if \ T(x) > \delta \\ p_{ij}^{t}, & otherwise \end{cases}$$
 (10)

This chaotic, binary flipping ensures each fox's position remains in the binary format required for feature selection.

Fitness evaluation of updated population:

After updating each fox position, the fitness function is recalculated for the new subset. For each fox P_i^{t+1} :

$$J(P_i^{t+1}) = Acc(P_i^{t+1}) - \lambda P_i^{t+1}$$
(11)

Where the classification accuracy using the subset of features measures $Acc(P_i^{t+1})$ indicated by P_i^{t+1} , and $|P_i^{t+1}|$ counts the selected features. The best fitness $J^*(S)$ observed so far is recorded, and the fox associated with this fitness is updated as the current best solution.

Convergence Criteria

The TM-RFO algorithm keeps switching between the exploration and exploitation stages until a halting condition is satisfied. Common standards consist of:

- The number of iterations reaches a maximum.
- The best fitness does not significantly improve over successive iterations.

When the algorithm converges, the solution with the highest fitness is chosen as the final subset of selected features.

Optimal feature subset

The final output is the feature subset S^* that yields the best fitness, balancing high classification accuracy with a minimal number of features. The final subset is expressed as,

$$S^* = \arg\max_{S \subset X} \left(Acc(S) - \lambda |S| \right)$$
 (12)

Where S^* is subsequently used in model training for classification task λ s, represents the regularization parameterbenefitting from reduced computational cost and improved interpretability.

Classification using DI-LSTM

The selected features are fed into the DI-LSTM model. The existing LSTMs [22] are a type of RNN designed to capture long-range dependencies in sequential data. Unlike traditional RNNs, LSTMs are better at retaining information over longer sequences due to their unique memory structure. Traditional LSTM networks [22] are optimized for handling sequential data, making them effective for such tasks; however, they contain numerous parameters due to their architecture, which includes input, forget, and output gates, along with cell states. The proposed deep neural network enhances this approach by incorporating DI-LSTMnetwork with four LSTM layers, followed by dropout regularization, a flattening layer, a fully connected (dense) layer, and an output layer for classification or regression. Fig 2 illustrates the construction of a deep neural networkarchitecture with DI-LSTM.

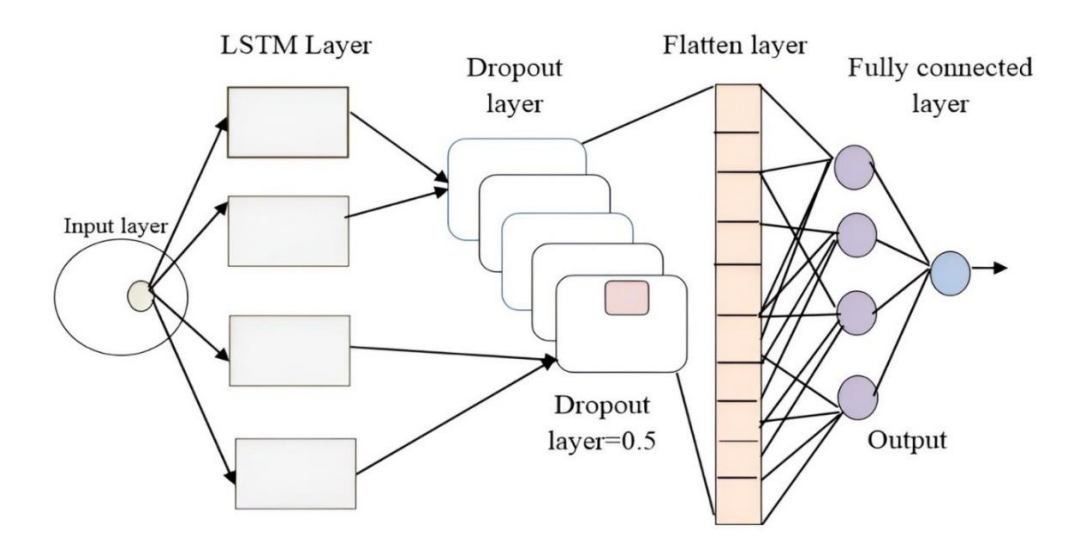


Fig 2: Deep Neural Network Architecture with Dropout Induced LSTM

Input layer

Let the selected features be represented as a vector $x_t \in \mathbb{R}^n$ at each time step t, where the number of selected features is n. These features are sequentially fed into the LSTM network over time.

LSTM Laver

An LSTM cell is made up of four main parts: the input gate, the output gate, the forget gate, and the cell state. Each LSTM cell uses the equations listed below to update its internal configuration and output at any given time:

a. Forget gate
$$f_t = \sigma \left(W_f . [h_{t-1}, x_t] + b_f \right) \tag{13}$$

Here, f_t decides which data from the prior cell state C_{t-1} should be kept. σ is the activation sigmoid function, W_f and b_f is the forget gate's weights and biases.

b. Input gate:

The input gate i_t selects which value should be changed in the cell state. It is calculated as:

$$i_{t} = \sigma(W_{i}.[h_{t-1}, x_{t}] + b_{i}) \tag{14}$$

Where x_t denotes the input at the current time step t, h_{t-1} the hidden state at the previous time step (t-1), and W_i the input gate's weight matrix. b_i Is the bias term for the input gate and σ stands for the sigmoid activation function.

c. Candidate cell state

The candidate cell state C_t introduces a collection of new values that can be added to the input gate-controlled cell state. It's computed as:

$$\widehat{C}_{t} = \tanh\left(W_{C} \cdot [h_{t-1}, x_{t}] + b_{c}\right) \tag{15}$$

Where \tanh is the hyperbolic tangent activation function, W_C is the weight matrix for generating the candidate cell state, b_C and is the bias term for the candidate cell state.

d. Cell state update

The cell state C_t is then updated by combining the previous cell state C_{t+1} and the candidate cell state \hat{C}_t , controlled by the forget gate f_t and input gate i_t . It is calculated as:

The cell state C_t is then updated by merging the previous C_{t+1} and candidate cell state \hat{C}_t , which are regulated by the forget gate f_t and input gate i_t . It's computed as:

$$C_{t} = f_{t} * C_{t-1} + i_{t} * \hat{C}_{t}$$
 (16)

Where *represents elements-wise multiplication. This equation allows the cell state to retain information as needed while incorporating new information.

e. Output gate

The output gate O_t determines whether aspects of the state of the cell should be transferred to the next hidden state. It's computed as:

$$o_{t} = \sigma(W_{o}.[h_{t-1}, x_{t}] + b_{o})$$
(17)

Where, W_o is the weight matrix for the output gate, h_{t-1} represents the hidden state at the previous time step (t-1), b_o and is the bias term for the output gate.

f. Hidden state

The hidden state h_t is updated by modifying the output gate o_t to the current cell state C_t . It is calculated as:

$$h_{t} = o_{t} * \tanh(C_{t}) \tag{18}$$

Where h_t represents the hidden state at a time step t, o_t represents the output gate value at the time step t, $\tanh(C_t)$ is the hyperbolic tangent function applied to the cell state at the time step t.



Dropout layer

Dropout regularization is applied after each LSTM layer to prevent overfitting. It randomly sets a fraction p of the input units to zero during training. Dropout maskis applied after each LSTM layer to prevent the network from becoming overly reliant on specific neurons. The mathematical operation for dropout at each time step is:

$$\hat{h}_{t} = M_{t}.h_{t} \tag{19}$$

Where, $M_t \sim Bernoull(p)$ is a binary mask with a probability p of retaining the neuron, h_t is the output of the LSTM layer, \hat{h}_t is the output after dropout.

Dense layer

The fully connected layer is used to transform the features extracted by the LSTM layers into the final output. For this layer, we have an input vector \hat{h} from the last LATM layer and it is mapped to an output vector using weight matrix W_d and bias vector by b_d .

$$y = W_d \cdot h_t + b_d \tag{20}$$

Where y represents the output of a neural network layer, W_d represents a weight matrix that connects the input h_t to the output y, b_d bias term that is added to the weighted sum of the inputs.

Output layer

For classification tasks, logits are transformed into probabilities by the output layer's softmax activation.

$$\widehat{\mathbf{y}} = soft \max(\mathbf{y}) \tag{21}$$

Where y represents the input to the softmax function, \hat{y} represents the output of a neural network layer.

Cardiac Disease Classification using T-ANFIS

The features extracted from an abnormal ECG signal are fed into the T-ANFIS to identify the specific type of cardiac disease. Traditional ANFIS models [23] merge neural networks with fuzzy logic, allowing them to effectively manage complex systems, including nonlinear relationships and uncertainties. However, conventional membership functions are predefined and may not adequately represent complex or unusual data distributions. While fuzzy logic offers some level of adaptability, it may not be sufficient for all data types. The proposed T-ANFIS utilizes trapezoidal membership functions that dynamically adjust their shapes based on the training data. By integrating machine learning techniques, T-ANFIS optimizes these parameters to enhance classification accuracy.

Input layer

The T-ANFIS system takes abnormal ECG data as input. These features are represented $X = \{x_1, x_2,x_n\}$, where each x_i represents features related to heart activity, Such as RR intervals, QRS duration, etc. These input features form the basis for diagnosing specific types of cardiac abnormalities.

Fuzzification layer

This layer utilizes membership functions to convert sharp input values into fuzzy values. In T-ANFIS, trapezoidal membership functions are used due to their ability to represent imprecise data effectively. The trapezoidal membership function for an input X can be defined as:



$$\mu_{A}(x) = \begin{cases} 0 & x \leq a \\ \frac{x-a}{b-c} & a < x \leq b \\ 1 & b < x \leq c \\ \frac{d-x}{d-c} & c < x \leq d \\ 0 & x \geq d \end{cases}$$

$$(22)$$

Where A is a fuzzy set defined by the parameters a, b, c, d?

Rule layer

This layer's nodes each stand for a fuzzy rule. Each node's output is calculated by multiplying its input membership values.

$$w_i = \mu_{Ai}(x_1) \mu_{Bi}(x_2) \tag{23}$$

Where w_i signifies the rule's firing strength i, $\mu_{Ai}(x_1)$ is amembership function for the variable x_1 in a fuzzy set A_i , $\mu_{Bi}(x_2)$ is amembership function for the variable x_2 in a fuzzy set B_i .

For the rules of the form:

$$R_i$$
: If x_1 is A_i and x_2 is B_i (24)

Normalization layer

The firing strengths w_i , from the previous layer are normalized to produce relative weights for each rule. The normalized firing strength \hat{w}_i is computed as:

$$\widehat{W}_i = \frac{W_i}{\sum_{j=1}^N W_j} \tag{25}$$

Where w_i represents the normalized or weighted value of w_i , w_i is the original value of the i^{th} element in a set of values. N Is the number of rules.

Defuzzification layer

This layer outputs the weighted consequence of each rule using a linear function of the inputs. For a given rule i, the defuzzified output z_i is defined as:

$$z_{i} = \widehat{w}_{i} \cdot (p_{i} x_{1} + q_{i} x_{2} + r_{i})$$
(26)

Where p_i, q_i , and r_i are the consequent parameters for the rule i.

Output laver

The sum of the contributions made by each rule produces the outcome:

$$F = \sum_{i=1}^{N} z_i = \sum_{i=1}^{N} \widehat{w}_i \cdot (p_i x_1 + q_i x_2 + r_i)$$
 (27)

This output F represents a continuous value that can be interpreted as the probability of a specific cardiac disease. The T-ANFIS modelutilizes the learned fuzzy rules to classify the input features such as normal, AFib, VFib, or Bradycardia.

RESULT AND DISCUSSION

The cardiac disease detection system based ondeepneural network model for DI-LSTM and the T-ANFIS has been verified. The performance of the suggested technique was compared to that of LSTM [22], ANN [24], and SVM [25]. The implementation results were generated using Intel Core i7 CPUs operating at 1.6 GHz and the Python platform.

Dataset description



This dataset contains images produced from ECG recordings and is specifically designed for the research of heart diseases. The images are classified according to various heart states, enabling for classification tasks and the study of cardiac diseases [28].

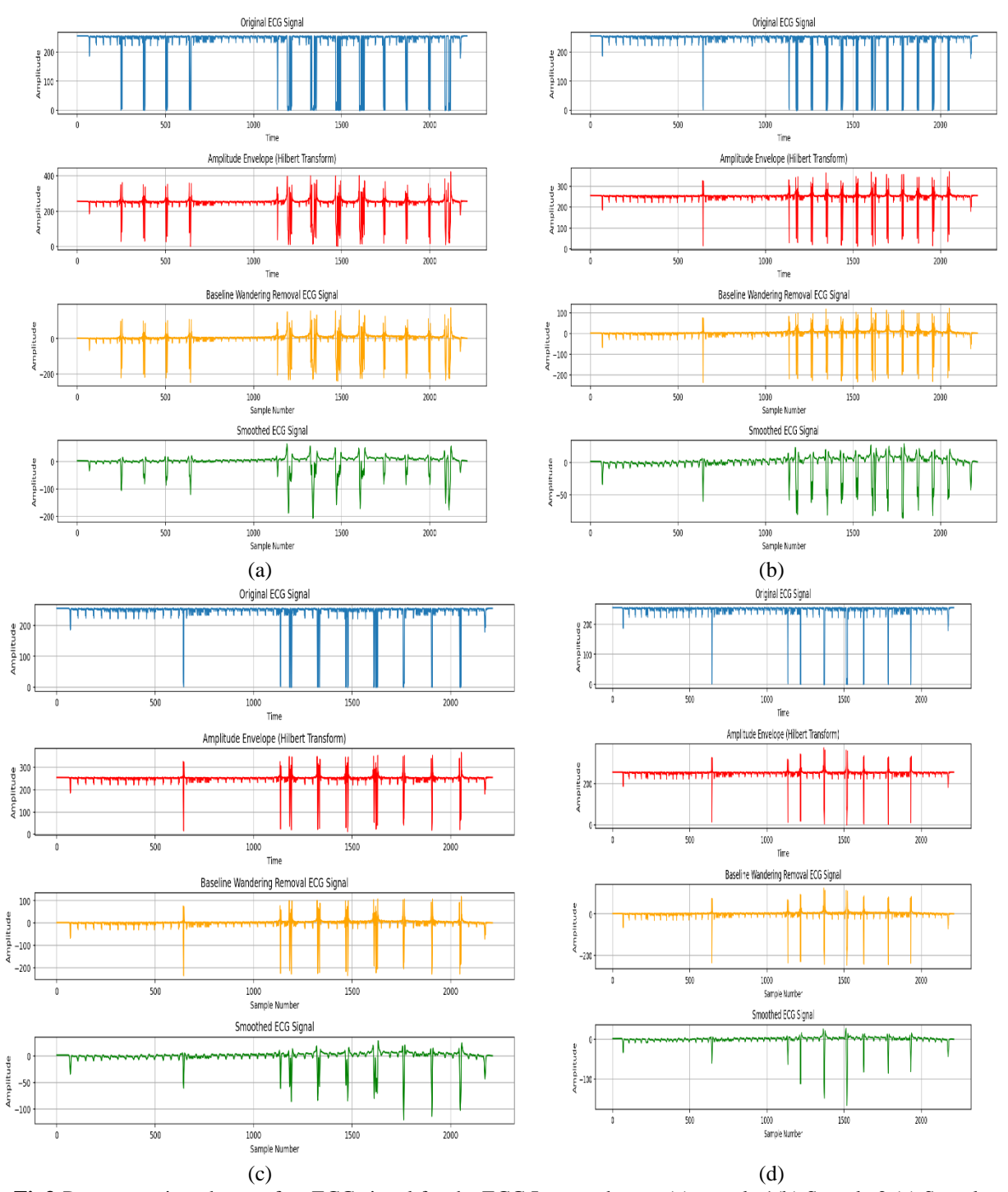


Fig3:Pre-processing phases of an ECG signal for the ECG Images dataset (a) sample 1(b) Sample 2 (c) Sample 3(d) Sample 4

Fig 3 illustrates the pre-processing stages of an ECG signal for the ECG Images dataset of Cardiac Patients analysis. The first plot shows the original ECG signal with its raw amplitude variations over time. The second plot presents the amplitude envelope of the ECG signal, extracted using the Hilbert Transform, which highlights the signal's amplitude variations more clearly, making it easier to analyze peak patterns. The third plot displays the ECG signal after baseline wandering removal, which corrects low-frequency shifts, stabilizing the baseline and improving signal clarity. The final plot shows the smoothed ECG signal, where noise and small fluctuations are reduced to provide a cleaner signal, emphasizing the primary waveform features critical for accurate feature extraction and further analysis.



ECG Arrhythmia Image Dataset

Arrhythmia ECG Using deep neural network architectures, image datasets have been used to investigate heartbeat categorization and observe some of the transfer learning capabilities. The signals match the heartbeat forms on an ECG in both normal and arrhythmia- and myocardial infarction-affected situations. Each segment of these pre-processed and segmented data represents a heartbeat [29].

Performance metrics

Performance can be assessed using a variety of criteria, including sensitivity, specificity, F1-score, accuracy, precision, recall, and recall. We employ the statistical indicators given in this section to evaluate the efficacy of our proposed approach. The metrics computed include true positive (TP), true negative (TN), false positive (FP), and false negative (FN).

Table 1 shows the computations for several performance metrics.

Table 2: Performance metrics

| Table 2: Performance metrics | | | | |
|------------------------------|----------------------------------------------------------------------|--|--|--|
| Performance Measures | Formula | | | |
| Accuracy | (TN + TP) | | | |
| | (TN + TP + FN + FP) | | | |
| Precision | TP | | | |
| | $\overline{ig(TP+FPig)}$ | | | |
| Recall | TP | | | |
| | $\overline{ig(TP+FPig)}$ | | | |
| F1-Score | $F = \frac{2PR}{P+R}$ | | | |
| | P+R | | | |
| Sensitivity | TP | | | |
| | $\overline{TP+FN}$ | | | |
| Specificity | TN | | | |
| | $\overline{TN+FP}$ | | | |
| AUC | 1 (TP TN) | | | |
| | $\frac{1}{2} \left(\frac{TP}{TP + FN} + \frac{TN}{TN + FP} \right)$ | | | |

Performance Evaluation for ECG Images Dataset

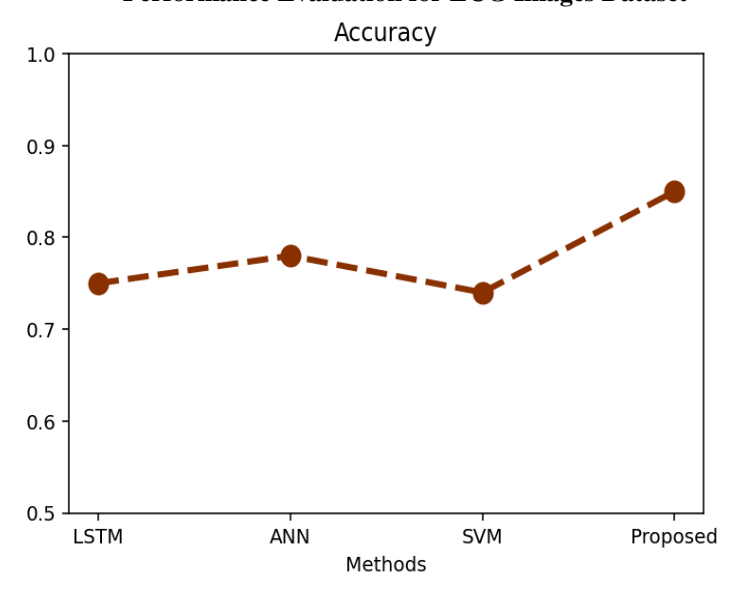


Fig 4: Comparison of the performance of accuracy for the ECG Images dataset

Fig 4 compares the proposed system's accuracy to existing approaches on the ECG Images dataset. The proposed technique achieved an accuracy of 87%, which outperformed ANN (76%), SVM (75%), and LSTM (71%). This demonstrates the

effectiveness of the proposed approach for classifying ECG pictures. Overall, the results show that the proposed technique is quite effective at diagnosing heart disorders.

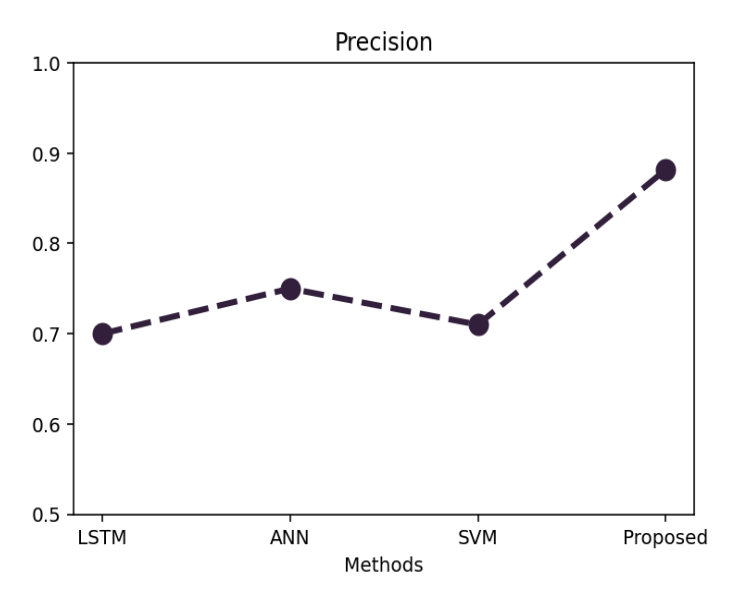


Fig 5: Comparison of the performance of precision for the ECG Images dataset

Fig 5 presents a comparison of the proposed system's accuracy against existing methods using the ECG Images dataset. The proposed system achieved an accuracy rate of 87%, outperforming LSTM (70%), ANN (75%), and SVM (71%). This demonstrates the proposed approach's ability to accurately identify positive cases in ECG image classification. Overall, the results emphasize the superior accuracy of the proposed methodology in diagnosing heart disease compared to traditional methods.

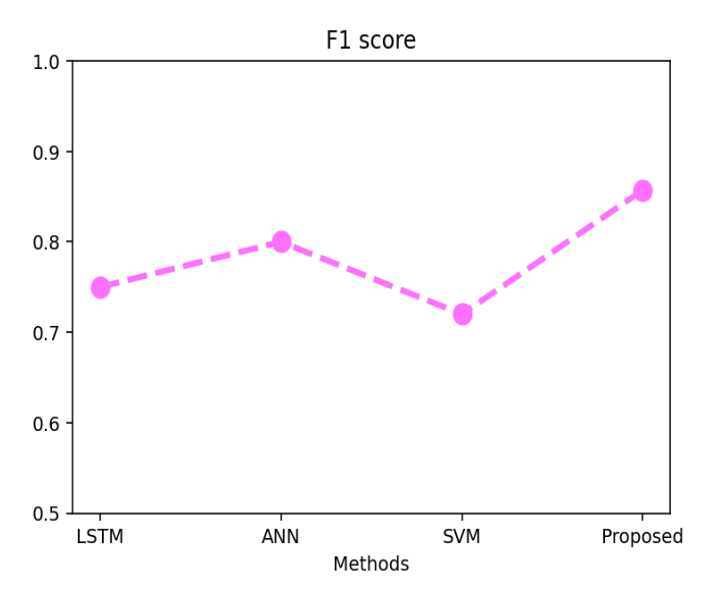


Fig 6: Comparison of the performance of F1-score for ECG Images dataset

Fig 6 compares the proposed system's F1 score to existing approaches on the ECG Images dataset. The suggested system obtained an exceptional F1 score of 86%, outperforming LSTM (75%), ANN (82%), and SVM (71%). This demonstrates the proposed method's solid balance of precision and recall in classifying ECG pictures. Overall, the data corroborate the proposed system's ability to effectively diagnose cardiac issues.

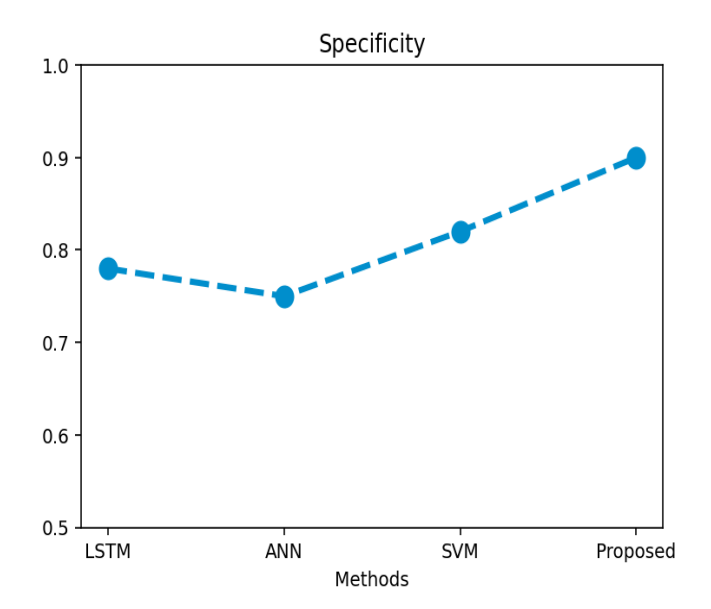


Fig 7: Specificity performance comparison for the dataset of ECG images

Fig 7 compares the suggested system's specificity with different methods using the dataset of ECG images. The proposed system achieves a notable specificity of 86%, exceeding the specificity scores of LSTM (78%), ANN (76%), and SVM (83%). This high specificity indicates the system's effectiveness in correctly identifying true negatives, which is crucial for accurately diagnosing cardiac conditions. Overall, the results emphasize the proposed system's advantage in minimizing false positive rates compared to existing approaches.

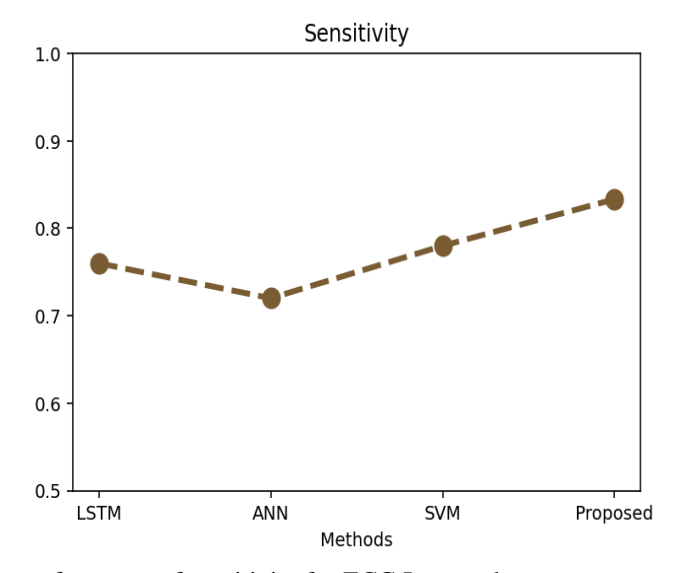


Fig 8: Comparison of the performance of sensitivity for ECG Images dataset

Fig 8 compares the proposed system's sensitivity to existing approaches on the ECG Images dataset. The proposed system attains a notable sensitivity of 82%, outpacing LSTM (76%), ANN (71%), and SVM (76%). This high sensitivity indicates the system's effectiveness in accurately identifying true positives, which is essential for detecting cardiac conditions. Overall, the results demonstrate the proposed system's superior performance in recognizing actual cases of heart disease compared to traditional methods.

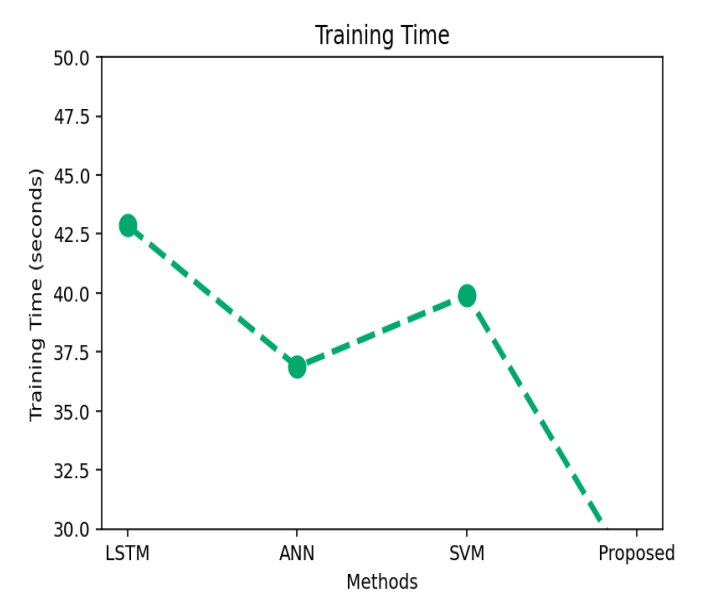


Fig: 9 Training time for ECG Images dataset

Fig 9 compares the training times of different methodson the ECG Images dataset in seconds. LSTM takes around 43 seconds, ANN approximately 41 seconds, SVM about 39 seconds, and the proposed method has the shortest training time at roughly 32 seconds. The trend shows a gradual decrease in training time from LSTM to the proposed method.

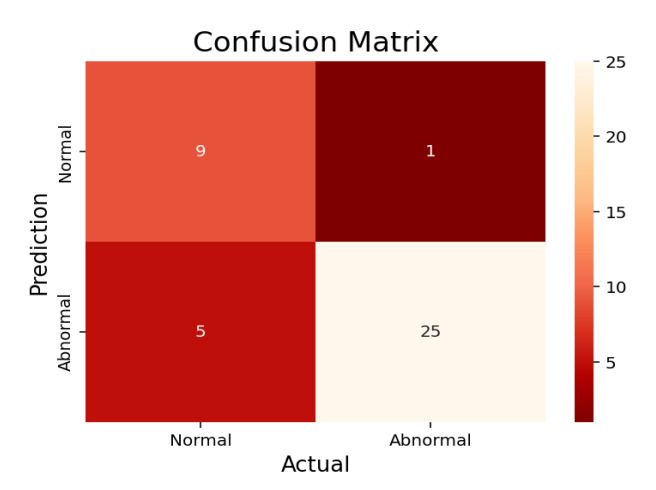


Fig: 10 Confusion matrix for ECG Images dataset

Fig 10 shows the performance of a classification model distinguishing between "Normal" and "Abnormal" cases. It correctly predicted 9 normal and 25 abnormal cases, with 5 normal cases misclassified as abnormal and 1 abnormal case misclassified as normal.

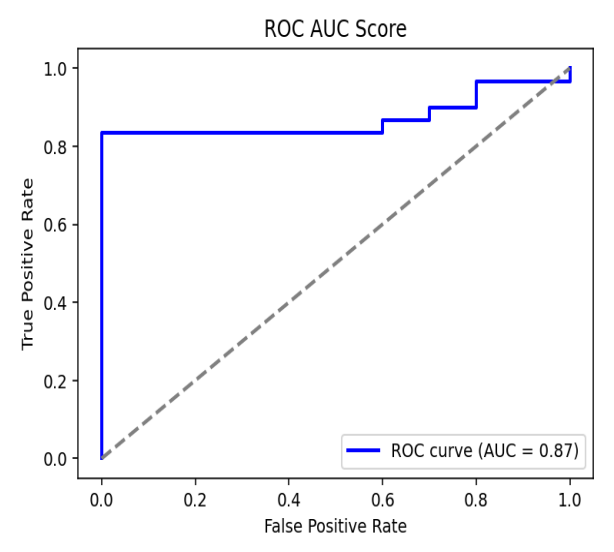


Fig: 11 ROC curve of AUC score for ECG Images dataset

The model achieves an AUC value of 87% on the ROC curve for the ECG Images dataset, as illustrated in Fig 11, indicating strong class discrimination. The curve shows strong classification capabilities, demonstrated by a high True Positive Rate (TPR) and a low False Positive Rate.

Performance Evaluation for ECG Arrhythmia Image Dataset

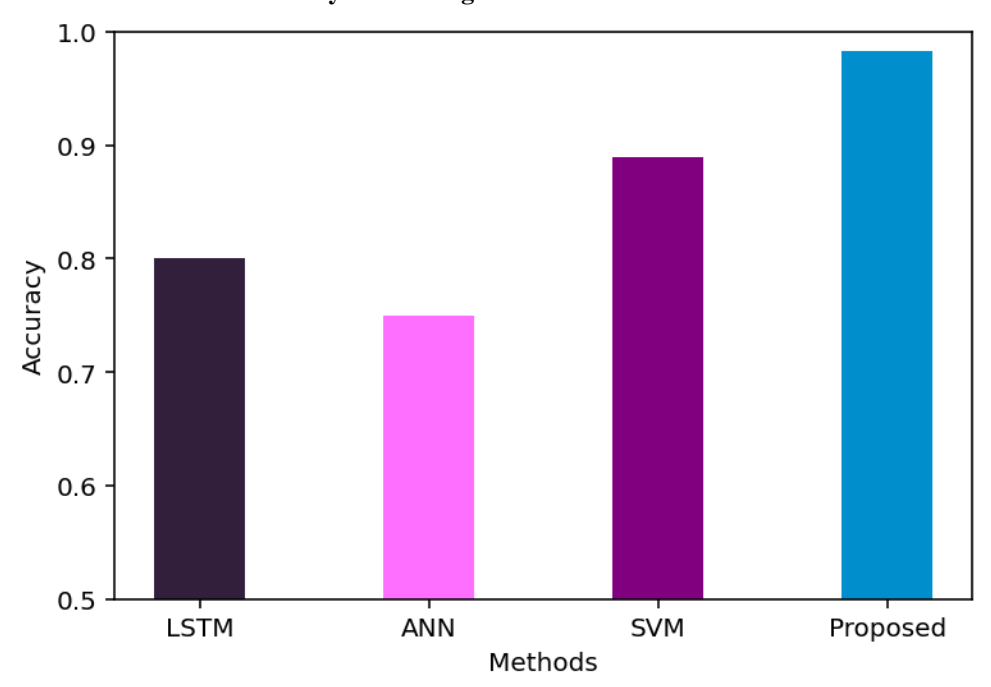


Fig 12: Comparison of the performance of accuracy for the ECG Arrhythmia Image dataset

Fig 12 utilizes the ECG Arrhythmia Image dataset to compare the accuracy of the suggested technique with alternative approaches. The suggested method outperforms LSTM (80%), ANN (75%), and SVM (89%), achieving an impressive accuracy of 98%. This outstanding result demonstrates how well the suggested technique works to identify arrhythmias in ECG images. The technique can produce very precise classifications in cardiac exams, according to the results overall.

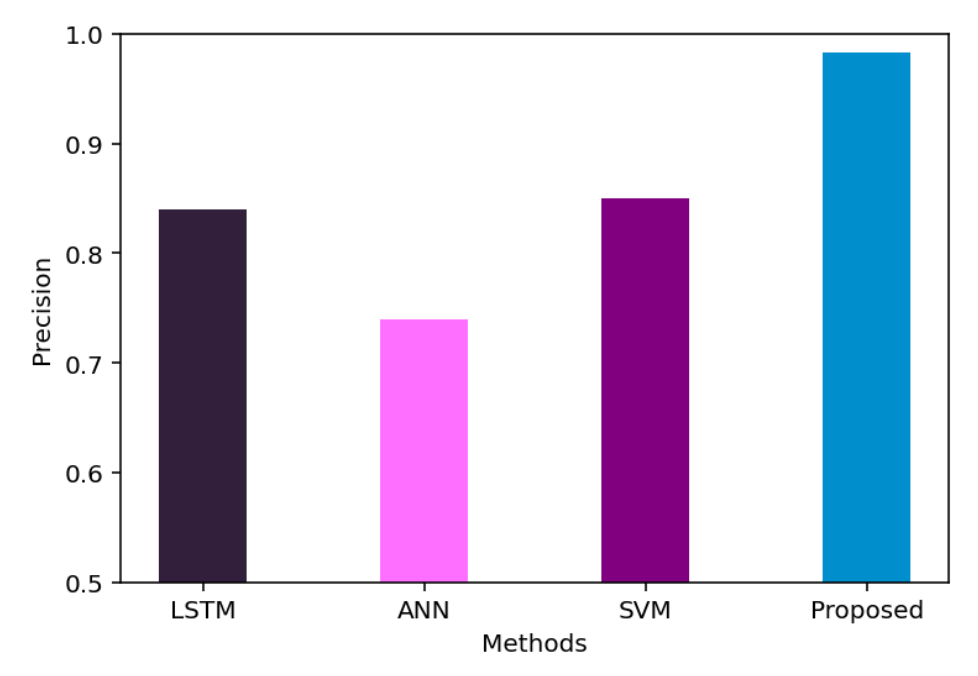


Fig13: Comparison of the performance of precision for ECG Arrhythmia Image Dataset

Fig 13 compares the precision of the proposed system against other methods using the ECG Arrhythmia Image dataset. The proposed system achieves an outstanding precision of 98%, significantly higher than LSTM (84%), ANN (74%), and SVM (85%). This highlights the proposed system's superior ability to accurately identify true positives in arrhythmia classifications.

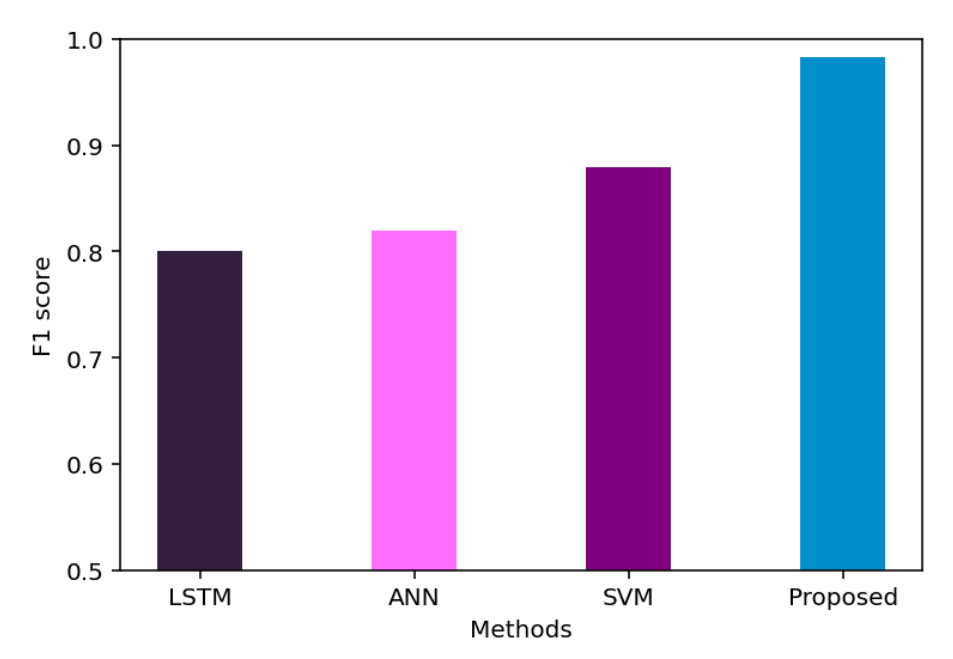


Fig 14: Comparison of the performance of F1-score for ECG Arrhythmia Image Dataset

Fig 14 compares the F1-score of the proposed system with other methods on the ECG Arrhythmia Image dataset. The proposed system achieves an impressive F1-score of 97%, significantly higher than LSTM (80%), ANN (82%), and SVM (88%). This exceptional score reflects the system's excellent balance of precision and recall in detecting arrhythmias. Overall, the results highlight the proposed method's superior performance in accurately classifying cardiac arrhythmias compared to existing approaches.

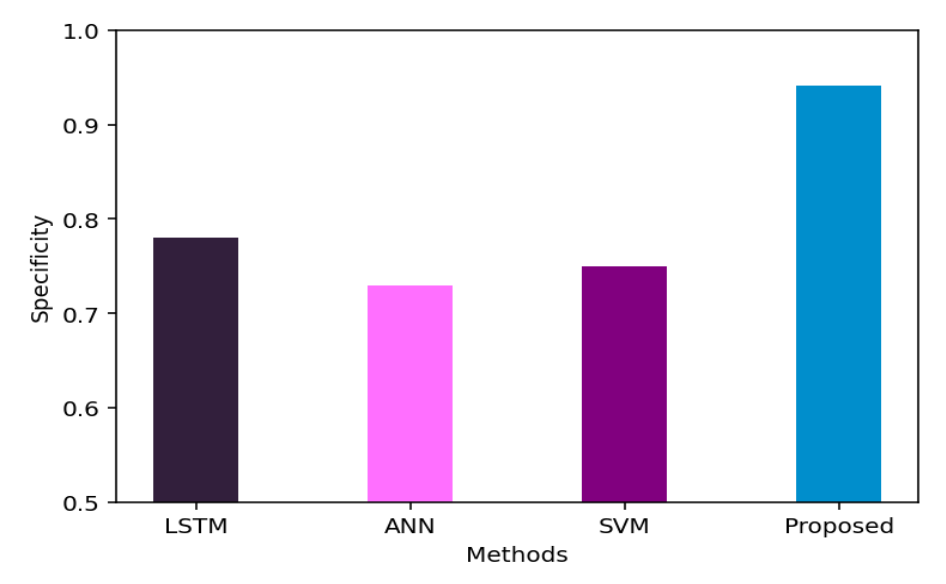


Fig15: Comparison of the performance of specificity for ECG Arrhythmia Image Dataset

Fig 15 compares the specificity of the proposed system with other methods using the ECG Arrhythmia Image dataset. The proposed system achieves an exceptional specificity of 94%, significantly higher than LSTM (78%), ANN (73%), and SVM (75%). This indicates the system's strong ability to accurately identify true negatives in arrhythmia classifications. Overall, the results highlight the proposed method's superior performance in reducing false positive rates compared to existing approaches.

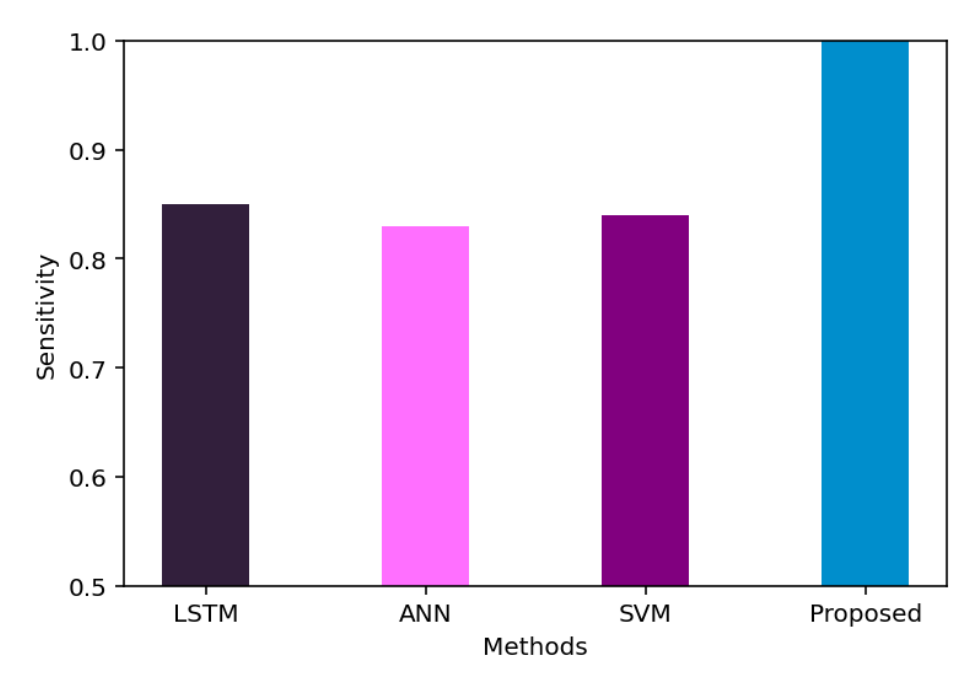


Fig16: Comparison of the performance of sensitivity for ECG Arrhythmia Image Dataset

Fig 16 compares the sensitivity of the proposed system with other methods using the ECG Arrhythmia Image dataset. The proposed system achieves an outstanding sensitivity of 99%, significantly higher than LSTM (85%), ANN (83%), and SVM (84%). This perfect sensitivity indicates the system's exceptional ability to accurately identify all true positives in arrhythmia detection. Overall, the results highlight the proposed method's superior performance in detecting cardiac arrhythmias compared to existing approaches.

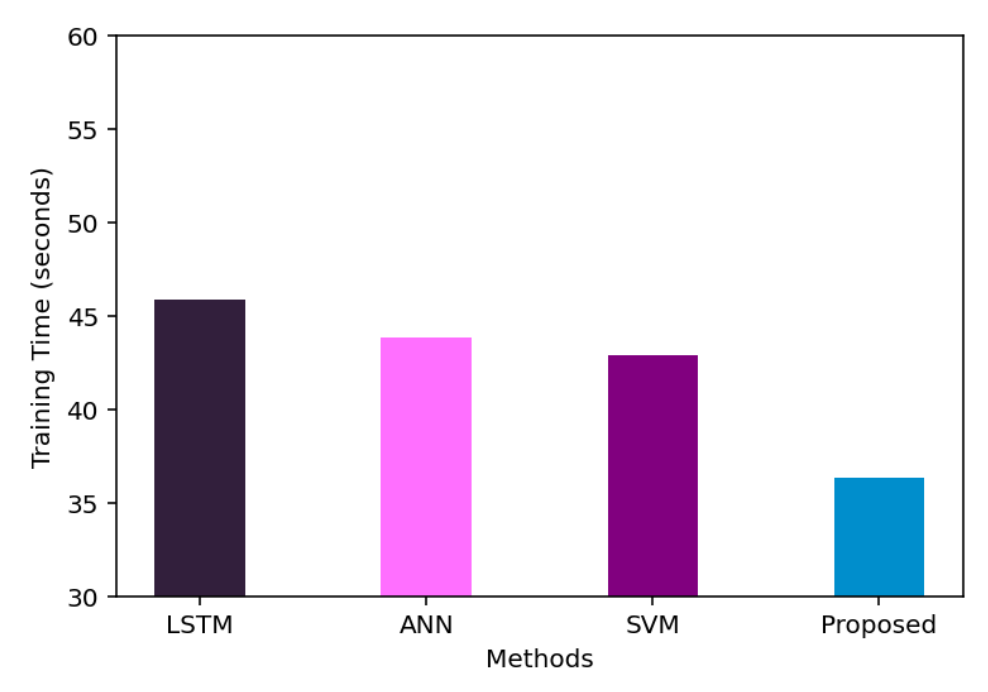


Fig: 17Training time for ECG Arrhythmia Image dataset

Fig 17 shows the training times of different methodsusing the ECG Arrhythmia Image dataset in seconds: LSTM takes approximately 45.86 seconds, ANN about 43.87 seconds, SVM around 42.91 seconds, and the proposed method achieves the lowest time at 36.31 seconds. The training time decreases progressively across the methods from LSTM to the proposed approach.

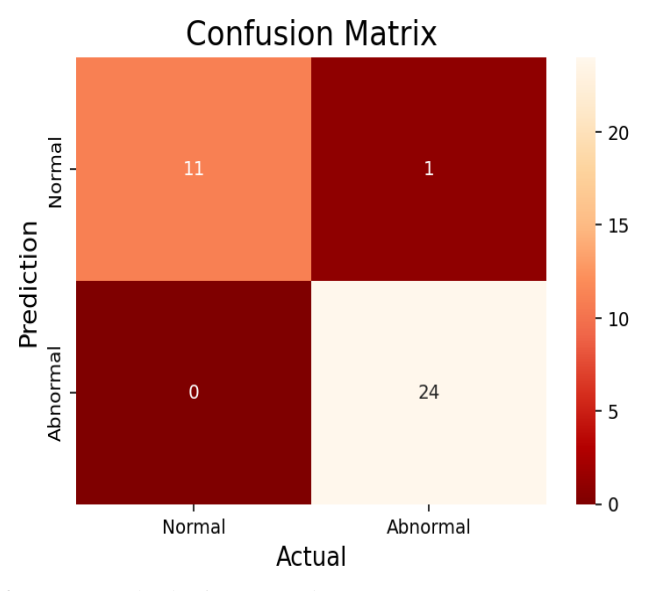


Fig: 18 Confusion matrix for ECG Arrhythmia Image dataset

Fig 18 shows the performance of a classification model distinguishing between "Normal" and "Abnormal" cases. It correctly predicted 11 normal and 24 abnormal cases, with 1 normal cases misclassified as abnormal and 0 abnormal cases misclassified as normal.

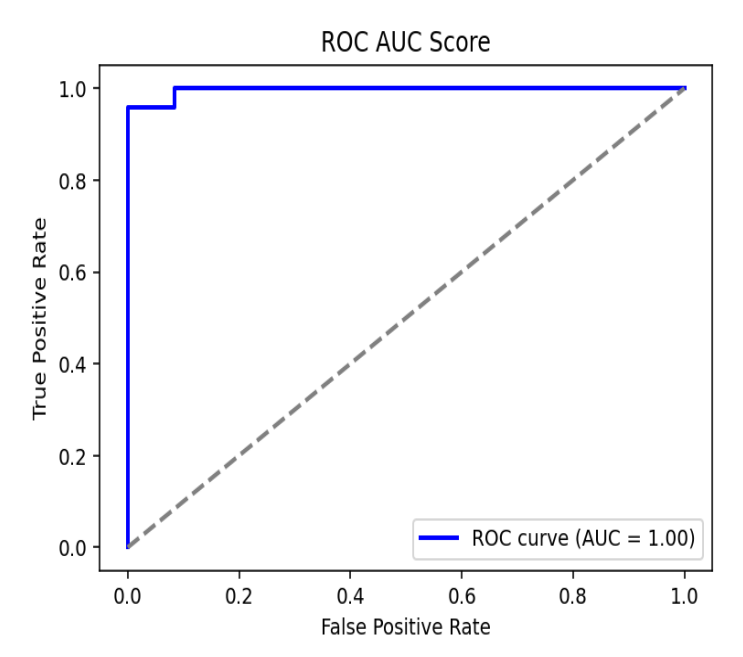


Fig: 19 ROC curve of AUC Score

Fig 19 displays the ROC curve for the ECG Arrhythmia Image dataset, where the model achieves a perfect AUC score of 100%, indicating excellent class classification. The curve demonstrates strong classification ability, characterized by a high True Positive Rate (TPR) and a low False Positive Rate (FPR).

Table 3: Performance Comparison of Classification Models

| | Performance metrics | | | | | | | |
|----------|---------------------|-----------|--------|-------|-------------|-------------|----------|--|
| | Accuracy | precision | Recall | F1- | Specificity | Sensitivity | Training | |
| Methods | | | | score | | | time | |
| LSTM | 80% | 84% | 77% | 80% | 78% | 85% | 45.86 | |
| ANN | 75% | 74% | 75% | 82% | 73% | 83% | 43.87 | |
| | | | | | | | | |
| SVM | 89% | 85% | 85% | 88% | 75% | 84% | 42.91 | |
| Proposed | 98% | 98% | 98% | 98% | 94% | 99% | 36.31 | |

Table 3 represents a comparison of four models—LSTM, ANN, SVM, and a proposed model across various performance metrics in a classification task. The proposed model outperforms the other models in terms of accuracy (98%), precision (98%), recall (98%), and F1 score (98%), indicating a strong balance between correctly identifying positive cases and minimizing false positives and negatives. It also achieves a higher specificity (94%) and sensitivity (99%), highlighting its ability to correctly classify both negative and positive cases. Notably, the proposed model also has the shortest training time (36.31 seconds), suggesting it is not only more accurate but also more computationally efficient than LSTM (45.86), ANN (43.87), and SVM (42.91). These results suggest the proposed model provides significant improvements in both predictive performance and training efficiency.

CONCLUSION

In conclusion, this paper presents an innovative T-ANFIS-based cardiac disease diagnosis system that efficiently processes ECG signals for identifying and classifying abnormal heartbeats. The integration of TM-RFO enhances feature selection by improving exploration capabilities, preventing premature convergence to local optima. The DL-LSTM model addresses the issue of overfitting in sequential data analysis by introducing dropout, leading to better generalization. The abnormal signals are further classified using the T-ANFIS model, which employs adaptive Trapezoidal membership functions, optimizing

their parameters for improved accuracy in detecting conditions such as Atrial Fibrillation, Ventricular Fibrillation, and Bradycardia. The proposed approach utilizes a T-ANFIS to improve the diagnosis of heart disease. Simulations were conducted using two datasets: the MIT-BIH dataset and ECG images specific to cardiac conditions. The results indicated that the T-ANFIS model outperformed existing models (LSTM, ANN, and SVM), achieving accuracy rates of 82%, 83%, and 82% on the ECG images related to cardiac diseases, and 97%, 97.4%, and 95% on the MIT-BIH dataset, respectively.

Declarations



Funding: This research article has not been funded by anyone.

Data availability: There is no data availability in this research.

Conflict of interest: All authors do not have any conflict of interest.

Ethical Approval: This article does not contain any studies with human participants or animals performed by any of the authors.

REFERENCE

- Wang, Zekai, Stavros Stavrakis, and Bing Yao.
 "Hierarchical Deep Learning with Generative
 Adversarial Network for Automatic Cardiac
 Diagnosis from ECG Signals." Computers in
 Biology and Medicine, vol. 155, 2023, p.
 106641.
- Khanna, Ashish, et al. "Internet of Things and Deep Learning Enabled Healthcare Disease Diagnosis Using Biomedical Electrocardiogram Signals." Expert Systems, vol. 40, no. 4, 2023, e12864.
- 3. Bensenane, Hamdan, et al. "A Deep Learning-Based Cardio-Vascular Disease Diagnosis System." *Indonesian Journal of Electrical Engineering and Computer Science*, vol. 25, no. 2, 2022, pp. 963–971.
- 4. Shin, Siho, et al. "Lightweight Ensemble Network for Detecting Heart Disease Using ECG Signals." *Applied Sciences*, vol. 12, no. 7, 2022, p. 3291.
- 5. Ahmed, Adel A., et al. "Classifying Cardiac Arrhythmia from ECG Signal Using 1D CNN Deep Learning Model." *Mathematics*, vol. 11, no. 3, 2023, p. 562.
- Sharada, K. A., et al. "High ECG Diagnosis Rate Using Novel Machine Learning Techniques with Distributed Arithmetic (DA) Based Gated Recurrent Units." *Microprocessors and Microsystems*, vol. 98, 2023, p. 104796.
- Rahman, M., et al. "Internet of Things Based Electrocardiogram Monitoring System Using a Machine Learning Algorithm." *International Journal of Electrical and Computer Engineering*, vol. 12, no. 4, 2022, pp. 3739– 3751.
- 8. Bhatia, Surbhi, et al. "Classification of Electrocardiogram Signals Based on Hybrid Deep Learning Models." *Sustainability*, vol. 14, no. 24, 2022, p. 16572.
- 9. Saini, Sanjeev Kumar, and Rashmi Gupta. "Artificial Intelligence Methods for the Analysis of Electrocardiogram Signals for Cardiac Abnormalities: State-of-the-Art and Future Challenges." *Artificial Intelligence Review*, vol. 55, no. 2, 2022, pp. 1519–1565.
- Aamir, Khalid Mahmood, et al. "Automatic Heart Disease Detection by Classification of Ventricular Arrhythmias on ECG Using

- Machine Learning." *Computers, Materials & Continua*, vol. 71, no. 1, 2022.
- 11. Zhang, Yuan, et al. "A CNN Model for Cardiac Arrhythmias Classification Based on Individual ECG Signals." *Cardiovascular Engineering and Technology*, 2022, pp. 1–10.
- 12. Rath, Adyasha, et al. "Improved Heart Disease Detection from ECG Signal Using Deep Learning Based Ensemble Model." *Sustainable Computing: Informatics and Systems*, vol. 35, 2022, p. 100732.
- 13. Sowmya, S., and Deepa Jose. "Contemplate on ECG Signals and Classification of Arrhythmia Signals Using CNN-LSTM Deep Learning Model." *Measurement: Sensors*, vol. 24, 2022, p. 100558.
- 14. Al-Issa, Yazan, and Ali Mohammad Alqudah. "A Lightweight Hybrid Deep Learning System for Cardiac Valvular Disease Classification." *Scientific Reports*, vol. 12, no. 1, 2022, p. 14297.
- 15. Aseeri, Ahmad O. "Uncertainty-Aware Deep Learning-Based Cardiac Arrhythmias Classification Model of Electrocardiogram Signals." *Computers*, vol. 10, no. 6, 2021, p. 82.
- 16. Karthik, S., et al. "Automated Deep Learning Based Cardiovascular Disease Diagnosis Using ECG Signals." *Computer Systems Science & Engineering*, vol. 42, no. 1, 2022.
- 17. Abubaker, Mohammed B., and Bilal Babayiğit. "Detection of Cardiovascular Diseases in ECG Images Using Machine Learning and Deep Learning Methods." *IEEE Transactions on Artificial Intelligence*, vol. 4, no. 2, 2022, pp. 373–382.
- 18. Mhamdi, Lotfi, et al. "Artificial Intelligence for Cardiac Diseases Diagnosis and Prediction Using ECG Images on Embedded Systems." *Biomedicines*, vol. 10, no. 8, 2022, p. 2013.
- 19. Daydulo, Yared Daniel, et al. "Cardiac Arrhythmia Detection Using Deep Learning Approach and Time-Frequency Representation of ECG Signals." *BMC Medical Informatics and Decision Making*, vol. 23, no. 1, 2023, p. 232.
- 20. Ram, R. Saravana, et al. "HybDeepNet: A Hybrid Deep Learning Model for Detecting Cardiac Arrhythmia from ECG Signals." *Information Technology and Control*, vol. 52, no. 2, 2023, pp. 433–444.
- 21. Bhuvaneshwari, M., et al. "Classification of SSVEP-EEG Signals Using CNN and Red Fox Optimization for BCI Applications." Proceedings of the Institution of Mechanical Engineers, Part H: Journal of Engineering in Medicine, vol. 237, no. 1, 2023, pp. 134–143.
- 22. Khan, Muhammad Ashfaq, and Yangwoo Kim.
 "Cardiac Arrhythmia Disease Classification
 Using LSTM Deep Learning Approach."

1 and JOURNAL OF RARE CARDIOVASCULAR DISEASE

- Computers, Materials & Continua, vol. 67, no. 1, 2021.
- 23. Khan, Mohammad Ayoub, and Fahad Algarni. "A Healthcare Monitoring System for the Diagnosis of Heart Disease in the IoMT Cloud Environment Using MSSO-ANFIS." *IEEE Access*, vol. 8, 2020, pp. 122259–122269.
- 24. Sarra, R. Rone, A. Musa Dinar, and M. Abed Mohammed. "Enhanced Accuracy for Heart Disease Prediction Using Artificial Neural Network." *Indonesian Journal of Electrical Engineering and Computer Science*, vol. 29, no. 1, 2023, pp. 375–383.
- 25. Jha, Chandan Kumar, and Maheshkumar H. Kolekar. "Cardiac Arrhythmia Classification Using Tunable Q-Wavelet Transform Based Features and Support Vector Machine Classifier." *Biomedical Signal Processing and Control*, vol. 59, 2020, p. 101875.
- 26. Zhou, S., and B. Tian. "Electrocardiogram Soft Computing Using Hybrid Deep Learning CNN-ELM." *Applied Soft Computing*, vol. 86, 2020, p. 105778.
- 27. Xu, Xue, Sohyun Jeong, and Jianqiang Li. "Interpretation of Electrocardiogram (ECG) Rhythm by Combined CNN and BiLSTM." *IEEE Access*, vol. 8, 2020, pp. 125380–125388.
- 28. Khan, Ali Haider, and Muzammil Hussain. "ECG Images Dataset of Cardiac Patients." *Mendeley Data*, V2, 2021, doi:10.17632/gwbz3fsgp8.2.
- 29. Daydulo, Yared Daniel, et al. "Cardiac Arrhythmia Detection Using Deep Learning Approach and Time-Frequency Representation of ECG Signals." BMC Medical Informatics and Decision Making, vol. 23, no. 1, 2023, p. 232.